

Electromagnetic ion temperature gradient modes of tearing mode parity in high β sheared slab plasmas

Zhe Gao^{a)}

Department of Engineering Physics, Tsinghua University, Beijing 100084, People's Republic of China

J. Q. Dong

Southwestern Institute of Physics, Chengdu 610041, People's Republic of China

G. J. Liu and C. T. Ying

Department of Engineering Physics, Tsinghua University, Beijing 100084, People's Republic of China

(Received 10 January 2002; accepted 28 February 2002)

The ion temperature gradient modes of tearing mode parity are investigated for arbitrary β ($=$ plasma pressure/magnetic pressure) plasmas in a sheared slab. Under the low β limit, the results agree with Reynders' conclusion that the lowest order ($l=1$) mode of tearing mode parity persists after the fundamental mode ($l=0$) of drift mode parity is completely stabilized by finite β [J. V. M. Reynders, *Phys. Plasmas* **1**, 1953 (1994)]. However, when the effects of the magnetic gradient drift and the coupling to the compressional Alfvén waves are included, the $l=0$ mode is more difficult to stabilize than the $l=1$ mode. It is also shown that the $l=1$ mode is much easier to stabilize by the magnetic shear than the $l=0$ mode. Generally, the $l=1$ mode grows faster in the low magnetic shear and low β regime while the $l=0$ mode is the dominant eigenmode of ion temperature gradient instability in high β plasmas. © 2002 American Institute of Physics. [DOI: 10.1063/1.1471516]

I. INTRODUCTION

The ion temperature gradient (ITG, η_i) modes have been considered as a candidate responsible for the anomalous ion transport in tokamak plasmas¹⁻³ and investigated in numerous theoretical studies.⁴⁻²⁰ Early analyses of the electrostatic modes^{1,4-9} established the basic stability property in very low β ($\beta=8\pi P/B^2 \ll m_e/m_i$) plasmas. Later, electromagnetic effects¹⁰⁻²⁰ were included to study the ITG mode with finite β modification. On the other hand, an integral approach^{8,9,16-19} was developed to throw off the long-wavelength restriction ($|k_\perp \rho_i| \ll 1$) that is necessary in the earlier differential approach.^{4-7,12}

In most of the previous studies, such as the first linear integral eigenmode study of the finite β modified ITG mode in a sheared slab performed by Dong *et al.*,¹⁷ only the fundamental ($l=0$) eigenmode of drift mode parity was considered, where l is the harmonic number of wave function in radial direction. Reynders¹⁹ derived the same eigenmode equation directly from the electromagnetic gyrokinetic equation and investigated the lowest order ($l=1$) eigenmode of tearing mode parity. He found that the $l=1$ eigenmode is more difficult to stabilize by finite β than the $l=0$ mode in the long poloidal wavelength (low k_y) regime and thus the $l=1$ mode persists after the $l=0$ mode is completely stabilized. In both of these studies, however, only the perturbations of the electrostatic potential, $\tilde{\phi}$, and the parallel vector potential, \tilde{A}_\parallel , were considered, while the perturbation of the perpendicular vector potential, \tilde{A}_\perp , was neglected. This is a good approximation only for low β plasmas. Moreover, the

magnetic gradient is needed to maintain pressure equilibrium for high β plasmas even in a slab.

Recently, Gao *et al.*²⁰ developed a set of integral equations to study drift instabilities in plasmas of arbitrary β values with a sheared slab magnetic configuration. Both components of the perturbed vector potential, \tilde{A}_\parallel and \tilde{A}_\perp , are considered together with $\tilde{\phi}$ in this full β model, as well as the magnetic gradient drift effects. The $l=0$ modes were analyzed and found to be unstable even at a high β , since β cannot effectively change the frequency and the particle-wave interaction in the lower frequency regime.

The $l=1$ mode is investigated in the present work with the full β model. The emphasis is placed on whether the $l=1$ mode still dominates in the low k_y regime in high β plasmas. The results are compared with those for the $l=0$ mode.

The organization of this paper is as follows. The basic integral eigenmode equations are presented in Sec. II. The numerical results and some analyses are described in Sec. III. Section IV is devoted to conclusions.

II. INTEGRAL EIGENMODE EQUATIONS

Consider a sheared magnetic field with a magnetic gradient $\mathbf{B}=B_0[\hat{z}(1+x/L_B)+\hat{y}(x/L_s)]$, where L_s and L_B are the scale lengths of the magnetic shear and the magnetic gradient, respectively. The magnetic gradient is included to maintain the pressure equilibrium for high β plasmas in a slab, so L_B is not independent of the pressure profiles, $L_n/L_B=\sum_{j=i,e}(\beta_j/2)(1+\eta_j)$. Here, $L_n^{-1}=- (1/n_j)dn_j/dx$, $\eta_j=d \ln T_j/d \ln n_j$, and $\beta_j=8\pi n_j T_j/B^2$. The equilibrium distributions for ions and electrons are f_{0j}

^{a)}Electronic mail: gaozhe97@mails.tsinghua.edu.cn

$= [n(X_{gj})/(\pi^{3/2}v_{ij}^3)] \exp(-v^2/v_{ij}^2)$, where $v_{ij} = \sqrt{2T_j(X_{gj})/m_j}$, $X_{gj} = x - v_y/\Omega_j$, and $\Omega_j = -q_j B/m_j c$.

We introduce three fluctuating scalar fields: $\tilde{\phi}$, $\tilde{A}_\parallel (= \tilde{\mathbf{A}} \cdot \hat{b})$, and $\tilde{A}_2 (= (\tilde{\mathbf{A}} \times \hat{e}_\perp) \cdot \hat{b})$, where all perturbed quantities have the form $\tilde{p}(\mathbf{r}, t) = p(x) \exp(ik_y y - i\omega t)$, $p(x) = 1/\sqrt{2\pi} \int p(k) \exp(ikx) dk$, $\hat{e}_\perp = \mathbf{k}_\perp / |\mathbf{k}_\perp|$, $\mathbf{k}_\perp = k_y \hat{y} + kx \hat{x}$, and $\hat{b} = \mathbf{B}/|B|$. For the fluctuations with $\omega \ll |\Omega_j|$ and $k_\perp \lambda_d \ll 1$, we have derived²⁰ the linear eigenmode equations as follows:

$$\sum_j \frac{q_j^2 n_0}{T_j} \left\{ \hat{\phi}(k) + \frac{1}{2\pi} \int dk' \int dx \exp[i(k' - k)x] \right. \\ \times \left[L_j(0,0,0,0) \hat{\phi}(k') + \frac{v_{ij}}{v_{te}} L_j\left(0,1, \frac{1}{2}, 0\right) \hat{A}_2(k') \right. \\ \left. \left. + \frac{v_{ij}}{v_{te}} L_j(0,0,0,1) \hat{A}_\parallel(k') \right] \right\} = 0, \quad (1)$$

$$\hat{A}_2(k) - \sum_j \frac{\beta_j}{2\pi b_j} \left\{ \int dk' \int dx \exp[i(k' - k)x] \right. \\ \times \left[\frac{v_{te}}{v_{ij}} L_j\left(1,0, \frac{1}{2}, 0\right) \hat{\phi}(k') + L_j(1,1,1,0) \hat{A}_2(k') \right. \\ \left. \left. + L_j\left(1,0, \frac{1}{2}, 1\right) \hat{A}_\parallel(k') \right] \right\} = 0, \quad (2)$$

$$\hat{A}_\parallel(k) - \sum_j \frac{\beta_j}{2\pi b_j} \left\{ \int dk' \int dx \exp[i(k' - k)x] \right. \\ \times \left[\frac{v_{te}}{v_{ij}} L_j(0,0,0,1) \hat{\phi}(k') + L_j\left(0,1, \frac{1}{2}, 1\right) \hat{A}_2(k') \right. \\ \left. \left. + L_j(0,0,0,2) \hat{A}_\parallel(k') \right] \right\} = 0. \quad (3)$$

Here,

$$L_j(m,n,s,l) = \left(\frac{-q_j}{|q_j|} \right)^{m+n} \int_0^{+\infty} dt t^s \exp(-t) \\ \times J_m(\sqrt{2b_j t}) J_n(\sqrt{2b'_j t}) \frac{\omega_{*j}}{\omega - \omega_{Djt}} K_{lj}, \quad (4)$$

$$K_{0j} = \left(\frac{\omega}{\omega_{*j}} - 1 \right) [\xi_j Z(\xi_j)] - \eta \left[\xi_j^2 + \left(\xi_j^2 - \frac{1}{2} \right) \xi_j Z(\xi_j) \right] \\ - \eta(t-1) [\xi_j Z(\xi_j)], \quad (5)$$

$$K_{1j} = \frac{k_\parallel}{|k_\parallel|} \xi_j \left[K_{0j} + \left(\frac{\omega_0}{\omega_{*j}} - 1 \right) - \eta(t-1) \right], \quad (6)$$

$$K_{2j} = \frac{k_\parallel}{|k_\parallel|} \xi_j K_{1j}, \quad (7)$$

$\omega_{*j} = (k_y T_j)/(\Omega_j m_j L_n)$, $\omega_{Djt} = -\omega_{*j} L_n/L_B$, $b_j = k_\perp^2 \rho_j^2/2$, $b'_j = k_\perp^2 \rho_j^2/2$, $\rho_j = v_{ij}/\Omega_j$, $\xi_j = (\omega - \omega_{Djt})/|k_\parallel| v_{ij}$, $k_\parallel = (x/L_s) k_y$, $k_\perp^2 = k_y^2 + k^2$, $k_\perp'^2 = k_y^2 + k'^2$, $\hat{\phi} = \phi$, $\hat{A}_2 = i v_{te} A_2/c$, $\hat{A}_\parallel = -v_{te} A_\parallel/c$, and $Z(\xi)$ is the plasma dispersion function.

This model is valid for plasmas of any β value, so we call it the full β model.²⁰ Omitting the coupling to the compressional Alfvén waves (CAWs) and the magnetic gradient effects, that is, $\hat{A}_2 = 0$ and $L_B \rightarrow \infty$, gives the low β model, which is valid for low β plasmas.

Equations (1)–(3) are the basic equations that govern the behavior of the modes, not only the lowest order mode but also the high order mode. As we know, the eigenfunctions from the differential approach are Hermite functions. The radial eigenmode order, l , is just the order of the Hermite function. In the integral approach, however, the number of l cannot be obtained directly from the equations, while different order modes exist in the different frequency regime, respectively. That is, different initial values induce the results of different orders.

III. NUMERICAL RESULTS

The integral equations, Eqs. (1)–(3), are solved using the Raleigh–Ritz technique. The detailed procedure is well documented in previous works^{20,21} and will not be repeated here.

The typical parameters^{8,17,19} chosen here are: $\eta_e = 2$, $\eta_i = 2$, $T_e/T_i = 1$, $m_i/m_e = 1836$, and $L_n/L_s = 0.025$ unless otherwise stated. For $\beta = 0$ and $k_y = 1$, the eigenfrequency of the $l=0$ mode is $(-0.40 + 0.38i)\omega_{*e}$ while that of the $l=1$ modes is $(-0.99 + 0.59i)\omega_{*e}$. For convenience, all the lengths have been normalized to $|\rho_i|$ in the following. In addition, all the results without otherwise statement are obtained from the full β model.

The definition and normalization in this work are the same as in Dong *et al.*¹⁷ although are somewhat different from those in Reynders.¹⁹ First, Reynders defined that $\beta = 4\pi n T_e/B^2$, so $(\beta)_{\text{Reynders}} = (\beta_e/2)_{\text{here}}$. Second, the parameter $k_y \rho_s$ in Sec. V of Ref. 19 was supposed to be $k_y^2 \rho_s^2$, although Reynders did not clearly clarify this point, or else the results of Reynders for the $l=0$ mode would be not consistent with those of Dong *et al.* Moreover, the definitions of thermal velocity in Ref. 19 and this work are different by a factor of $\sqrt{2}$, so the relation exists in a $T_e/T_i = 1$ plasma, $(k_y \rho_s)_{\text{Reynders}} = (k_y^2/2)_{\text{here}}$.

Figure 1 shows the real frequencies and growth rates for the $l=0$ and $l=1$ mode as functions of β_e with $k_y = 1$, i.e., $(k_y \rho_s)_{\text{Reynders}} = 0.5$ in Ref. 19. The results from the low β model are consistent with Reynders' results.¹⁹ The $l=1$ mode demonstrates a large growth rate at low β values and is stabilized before the $l=0$ mode is when β increases. This conclusion is still valid in the full β model. The full β effects, including the magnetic gradient drift effects and the coupling to A_2 , strengthen the stabilization effect of finite β on the $l=1$ mode but reduce it on the $l=0$ mode. The results also verify the stabilizing mechanism discussed in Ref. 20. An increasing β reduces the frequency and then the growth rate through reducing the inverse Landau damping. This β effect, however, is weakened at the low frequency regime. The $l=0$ mode cannot be stabilized, since the frequency de-

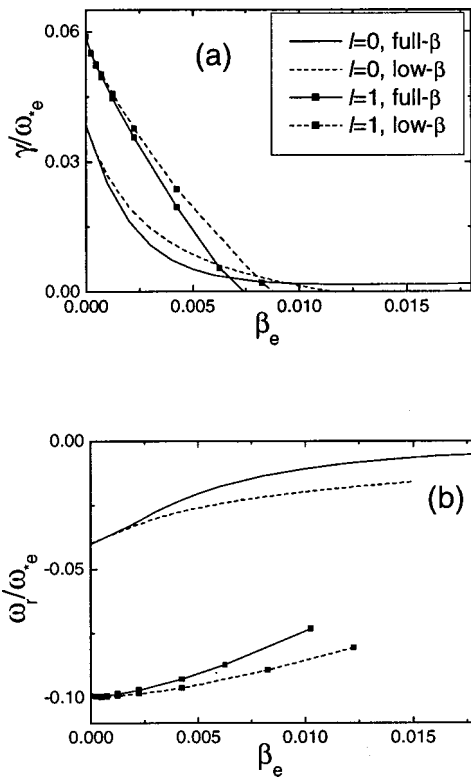


FIG. 1. Mode growth rate (a) and frequencies (b) of both the $l=0$ and $l=1$ modes as a function of β_e for $\eta_i = \eta_e = 2.0$, $m_i/m_e = 1836$, $\beta_e = \beta_i$, $L_n/L_s = 0.025$, and $k_y = 1$. The solid and dashed lines denote the results from the full β model and the low β model, respectively. The lines with squares denote the $l=1$ mode and the lines without symbols denote the $l=0$ mode.

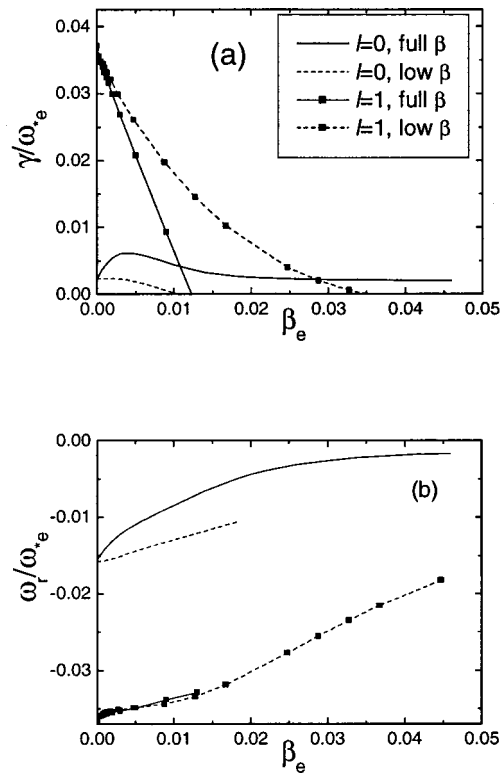


FIG. 2. The same as Fig. 1 except for $k_y = 0.35$.

increases to a very low level soon and flattens when β increases in the full β model. However, the $l=1$ mode has so high a frequency that β stabilizes the mode before reducing the frequency to a low level. For the $l=1$ mode, therefore, the inclusion of the full β effects strengthens the finite β stabilization effect.

With $k_y = 0.35$, the real frequencies and growth rates for the $l=0$ and $l=1$ modes are shown as functions of β_e in Fig. 2. In the low β model, the $l=1$ mode not only grows faster than the $l=0$ mode does but also is stabilized after the $l=0$ mode is. It is noted that the mode with $k_y = 0.35$ here is identical with that with $(k_y \rho_s)_{\text{Reynders}} = 0.06125$ in Ref. 19. Compared to the results shown in Fig. 4 of Ref. 19, the low β results here are consistent with Reynolds' results.¹⁹ For example, at $k_y = 0.35$ and $\beta_e = 0.01$, i.e., $(k_y \rho_s)_{\text{Reynders}} = 0.06125$ and $(\beta)_{\text{Reynders}} = 0.005$, both calculations give an eigenfrequency of about $(-0.034 + 0.018i)\omega_{*e}$. However, using the full β model, we can see that the $l=1$ mode is stabilized at a low β value while the $l=0$ mode still cannot be stabilized. The mechanism is the same as that with $k_y = 1$ described in the above paragraph.

Figure 3 depicts the growth rates and frequencies of the $l=1$ mode as functions of k_y for different values of β . The $l=1$ modes, with the typical parameter, are completely stabilized with a β above about 3%. The same plot for the $l=0$ mode is shown in Ref. 20. It is recalled that the $l=0$ mode remains unstable until $\beta > 10\%$ although the growth rate is very low.

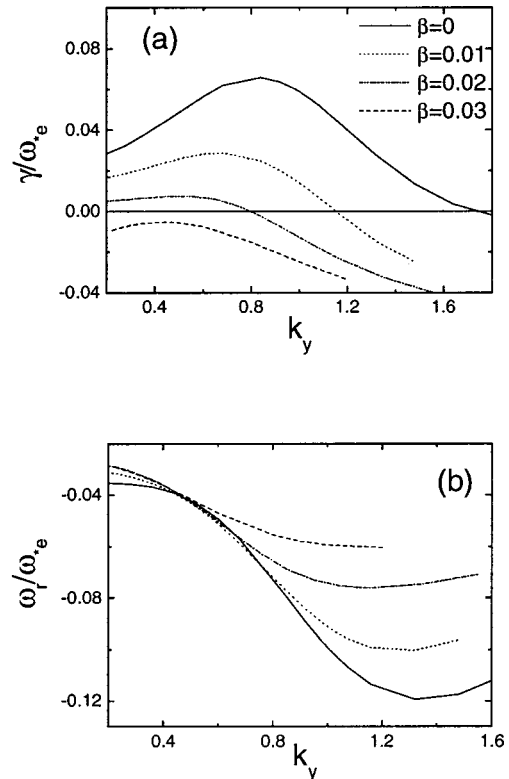


FIG. 3. Mode growth rate (a) and frequencies (b) of the $l=1$ mode as a function of k_y for $\beta = 0, 0.01, 0.02$, and 0.03 , respectively. The other parameters are the same as for Fig. 1.

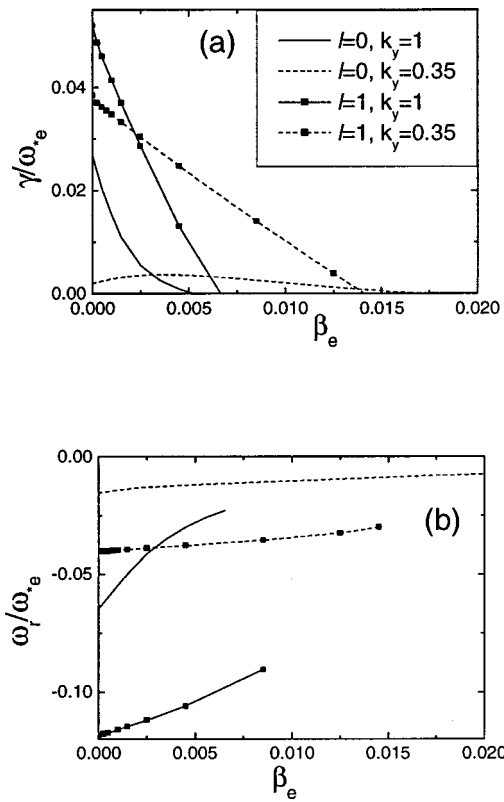


FIG. 4. Mode growth rate (a) and frequencies (b) of both the $l=0$ and $l=1$ modes with $\eta_e=0.4$ as a function of β_e for $k_y=1$ and 0.35, respectively. All the results are from the full β model. The solid and dashed lines denote the results for $k_y=1$ and 0.35, respectively. The other parameters and denotations are the same as for Fig. 1.

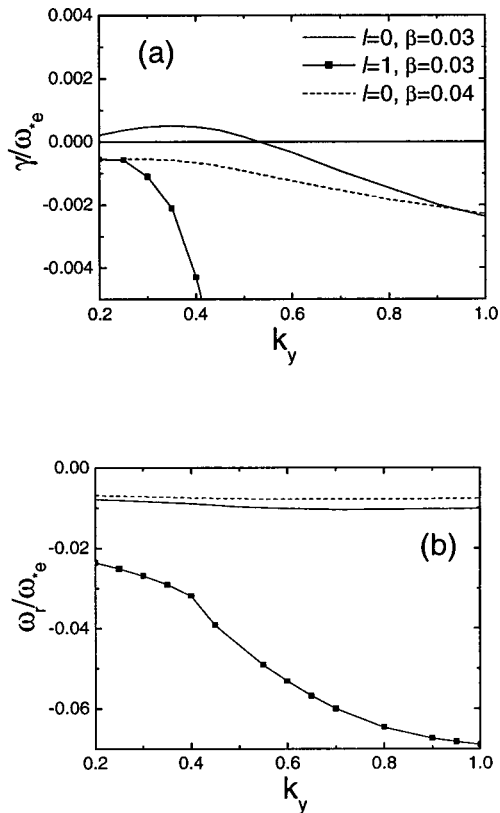


FIG. 5. Mode growth rate (a) and frequencies (b) of the $l=0$ and $l=1$ mode as a function of k_y for $\beta=0.03$ and 0.04, respectively. The other parameters are the same as for Fig. 1 except for $\eta_e=0.4$.

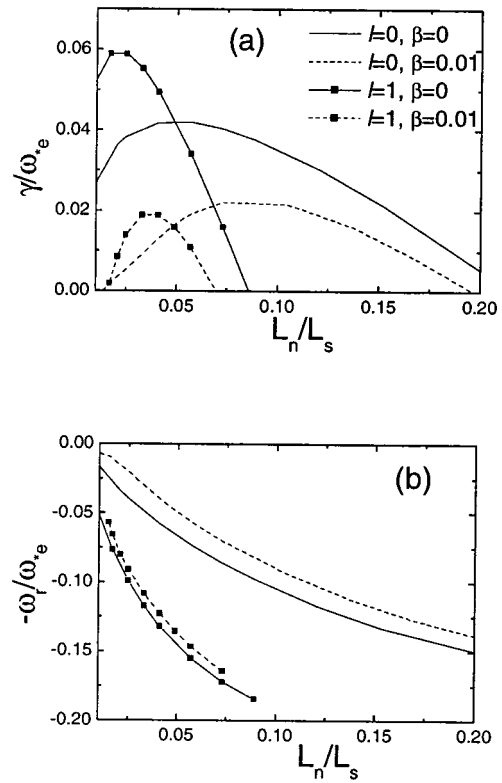


FIG. 6. Mode growth rate (a) and frequencies (b) of both the $l=0$ and $l=1$ modes as a function of L_n/L_s for $k_y=1, \beta=0$ and 0.01, respectively. The solid and dashed lines denote the results for $\beta=0$ and 0.01, respectively. The other parameters and denotations are the same as for Fig. 1.

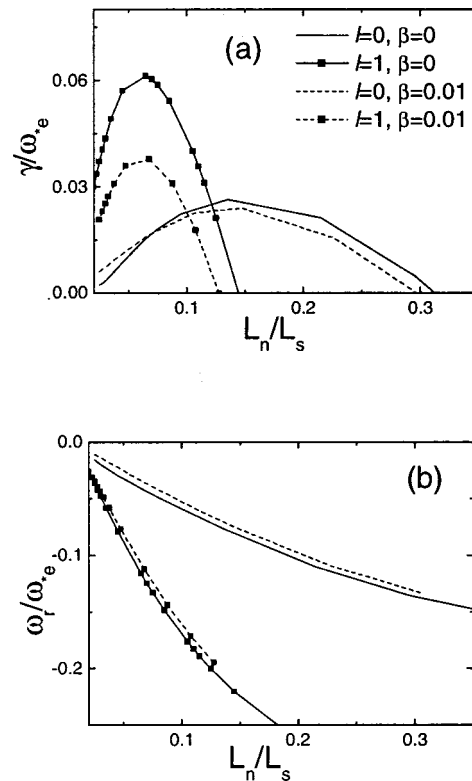


FIG. 7. The same as Fig. 6 except for $k_y=0.35$.

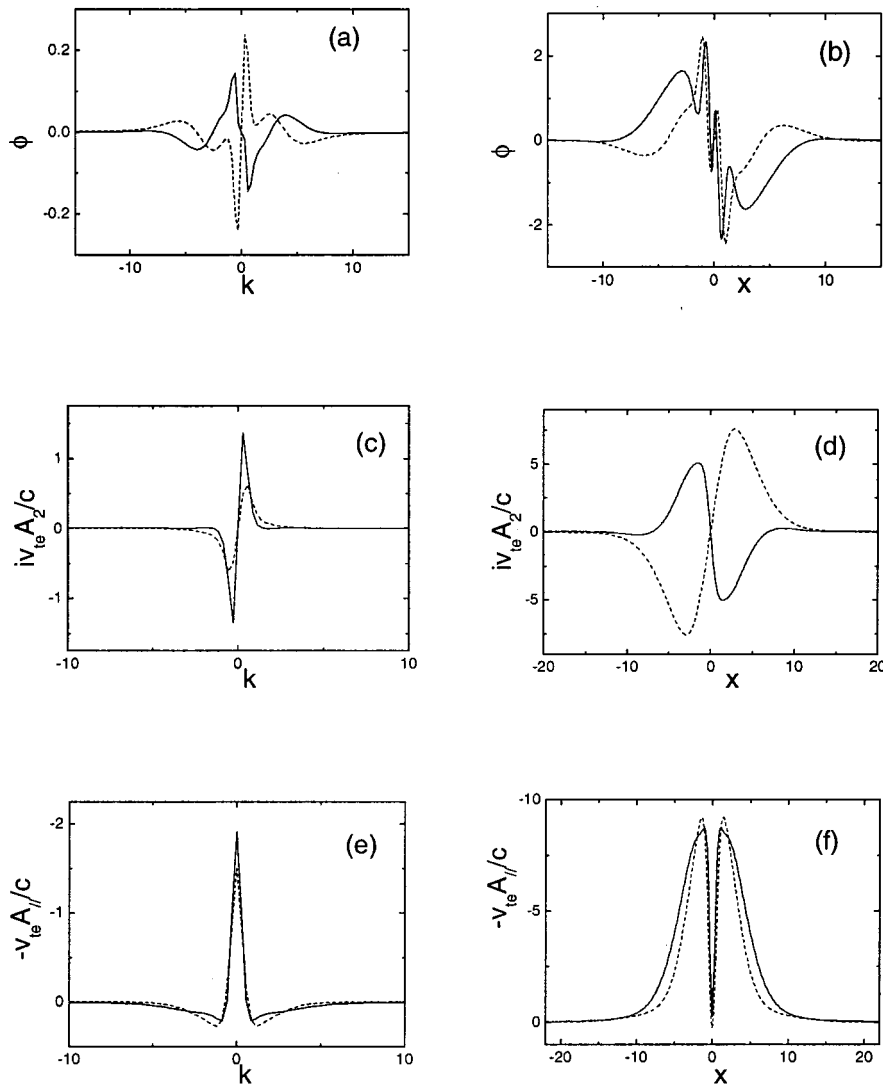


FIG. 8. Structure of the $l=1$ eigenmode: (a) $\phi(k)$ vs k ; (b) $\phi(x)$ vs x ; (c) $A_2(k)$ vs k ; (d) $A_2(x)$ vs x ; (e) $A_{\parallel}(k)$ vs k ; (f) $A_{\parallel}(x)$ vs x for $\beta=0.01$ and $k_y=0.35$. The solid and dashed lines denote the real and imaginary parts. The other parameters are the same as in Fig. 1.

With the above typical parameters, in fact, the $l=0$ mode is still unstable even when β reaches a very high value. However, we had shown²⁰ that the $l=0$ mode could be stabilized by finite β when η_e is less than 1.0 and other parameters are unaltered. With $\eta_e=0.4$, the real frequencies and growth rates for $l=0$ and $l=1$ modes are shown in Fig. 4 as functions of β with $k_y=1$ and 0.35, respectively. Here, all the results are from the full β model. The η_e affects the stable property of the $l=0$ mode while hardly change the property of the $l=1$ mode with a high frequency. With $k_y=1$, the $l=0$ mode is stabilized even before the $l=1$ mode is; while, with $k_y=0.35$, the $l=0$ mode is stabilized still after the $l=1$ mode is. It is known that the mode with a lower k_y has a much lower frequency. So, even though the $l=0$ mode with a low k_y can be stabilized by finite β , the stabilization will be difficult. Figure 5 shows the k_y spectra of $l=0$ and $l=1$ modes with $\eta_e=0.4$. When β reaches 3%, the $l=1$ mode is completely stabilized while the $l=0$ mode is still unstable in the low k_y regime. The complete stabilization of the $l=0$ mode needs a higher β .

Besides the β , the magnetic shear is known²⁰ as another stabilizing factor for the ITG mode even in the high β regime. Figures 6 and 7 show the real frequency and growth

rates for the $l=0$ and $l=1$ mode as functions of L_n/L_s with $k_y=1.0$ and 0.35, respectively. The $l=1$ mode is easier to be stabilized by magnetic shear than the $l=0$ mode for both $k_y=1.0$ and 0.35 though a lower k_y mode needs a stronger shear. Then, the $l=1$ mode exists and dominates in the low magnetic shear and low β regime. For tokamak plasmas, the low shear regime usually exist in the interior, at the same time, the interior is the high β regime. So the $l=0$ eigenmode is the dominant ITG mode in the high β tokamak-type plasmas.

The $l=1$ eigenmode structures for $k_y=0.35$ are shown in Fig. 8. The $l=1$ mode exhibits a tearing mode parity; ϕ and A_2 have odd parity, while A_{\parallel} has even parity. The structures of $\phi(x)$ and $A_{\parallel}(x)$ from the full β model are similar with the structures shown by Reynders.¹⁹ The perturbations in k space, especially $\phi(k)$, extend to the $k \geq 1$ regime. It is the cause of the fine-scale structure near the rational surface in x space mentioned by Reynders.¹⁹ This fine structure could not be seen in the differential approach.

The $l=2$ mode (the second order mode with drift mode parity) and $l=3$ mode (the second order mode with tearing mode parity) are also investigated using the full β model.

They have higher frequencies and are damped by either β or L_n/L_s before the $l=0$ and $l=1$ modes.

IV. CONCLUSIONS

The $l=1$ mode, the lowest order eigenmode of tearing mode parity, is investigated using the model for arbitrary β in a sheared slab. Under the low β limit, the results agree with Reynders' conclusion¹⁹ that the $l=1$ mode persists after the $l=0$ mode is completely stabilized by finite β . However, when the effects of the magnetic gradient drift and the coupling to A_2 are included, the $l=0$ mode is more difficult to stabilize than the $l=1$ mode, though the $l=1$ mode demonstrates a larger growth rate in the low β regime. The results are consistent with the stabilization mechanism discussed in Ref. 20, that is, an increasing β reduces the frequency and then the growth rate through reducing the inverse Landau damping and this β effect is weakened at the low frequency regime.

In addition, the magnetic shear stabilization effect is also studied for the $l=0$ and $l=1$ modes. It is shown that the $l=1$ mode is much easier to be stabilized by magnetic shear than the $l=0$ mode. In conclusion, the $l=1$ mode grows faster in the low magnetic shear and low β regime while the $l=0$ mode is the dominant eigenmode of ITG instability in high β plasmas.

The present study was performed in the slab geometry and then did not consider the effects of curvature drift and trapped electrons. These effects have already been considered in some previous studies^{18,22,23} for the $l=0$ mode and shown to be likely important in a torus in affecting the ion temperature gradient instability. However, it is still an unexplored topic for the $l=1$ mode of tearing mode parity and will be studied in the future work.

ACKNOWLEDGMENTS

This work was supported by the National Science Foundation of China, Grants Nos. 19889506 and 10135020.

- ¹B. Coppi, M. N. Rosenbluth, and R. Z. Sagdeev, *Phys. Fluids* **10**, 582 (1967).
- ²M. Greenwald, D. Gwinn, S. Milora, J. Parker, R. Parker, S. Wolfe, M. Besen, F. Camacho, S. Fairfax, C. Fiore, M. Foord, R. Gandy, C. Gomez, R. Granetz, B. La Bombard, B. Lipschultz, B. Lloyd, E. Marmor, S. McCool, D. Pappas, R. Petrasso, P. Pribyl, J. Rice, D. Schuresko, Y. Takase, J. Terry, and R. Watterson, *Phys. Rev. Lett.* **53**, 352 (1984).
- ³S. D. Scott, P. H. Diamond, R. J. Fonck, R. B. Howell, K. P. Jahnig, G. Schilling, E. J. Synakowski, M. C. Zarnstorff, C. E. Bush, E. Fredrickson, K. W. Hill, A. C. Janos, D. K. Mansfield, D. K. Owens, H. Park, G. Pautasso, A. T. Ramsey, J. Schivell, G. D. Tait, W. M. Tang, and G. Taylor, *Phys. Rev. Lett.* **64**, 531 (1990).
- ⁴W. M. Tang, *Nucl. Fusion* **18**, 1089 (1978).
- ⁵F. Romanelli, *Phys. Fluids B* **1**, 1018 (1989).
- ⁶T. S. Hahn and W. M. Tang, *Phys. Fluids B* **1**, 1185 (1989).
- ⁷M. Artun and W. M. Tang, *Phys. Fluids B* **4**, 1102 (1992).
- ⁸R. Linsker, *Phys. Fluids* **24**, 1485 (1981).
- ⁹J. Q. Dong, W. Horton, and J. Y. Kim, *Phys. Fluids B* **4**, 1867 (1992).
- ¹⁰Y.-K. Pu and S. Migliuolo, *Phys. Fluids* **28**, 1722 (1985).
- ¹¹Z. Gao, J. Q. Dong, G. J. Liu, and C. T. Ying, *Phys. Plasmas* **8**, 2816 (2001).
- ¹²S. Migliuolo, *Phys. Fluids* **30**, 922 (1987).
- ¹³A. Jarmen, P. Anderson, and J. Weiland, *Nucl. Fusion* **27**, 941 (1987).
- ¹⁴J. Weiland and A. Hirose, *Nucl. Fusion* **32**, 151 (1992).
- ¹⁵B. G. Hong, W. Horton, and D. I. Choi, *Plasma Phys. Controlled Fusion* **31**, 1291 (1989).
- ¹⁶W. Horton, J. E. Sedlak, D.-I. Choi, and B. G. Hong, *Phys. Fluids* **28**, 3050 (1985).
- ¹⁷J. Q. Dong, P. N. Guzdar, and Y. C. Lee, *Phys. Fluids* **30**, 2694 (1987).
- ¹⁸J. Y. Kim, W. Horton, and J. Q. Dong, *Phys. Fluids B* **5**, 4030 (1993).
- ¹⁹J. V. M. Reynders, *Phys. Plasmas* **1**, 1953 (1994).
- ²⁰Z. Gao, J. Q. Dong, G. J. Liu, and C. T. Ying, *Phys. Plasmas* **9**, 569 (2002).
- ²¹J. Q. Dong, P. N. Guzdar, and Y. C. Lee, *Phys. Fluids* **30**, 399 (1987).
- ²²G. Rewoldt and W. M. Tang, *Phys. Fluids B* **2**, 318 (1990).
- ²³J. Q. Dong and W. Horton, *Phys. Fluids B* **5**, 1581 (1993).